iScience, Volume *23*

Supplemental Information

Preferential Perinatal Development of Skin-Homing NK1.1^{+} Innate Lymphoid Cells for Regulation of Cutaneous Microbiota Colonization

Jie Yang, Katherine H. Restori, Ming Xu, Eun Hyeon Song, Luming Zhao, Shaomin Hu, Pingyun Lyu, Wei-Bei Wang, and Na Xiong

SUPPLEMENTAL INFORMATION

Table S1. Summary of surface and intracellular molecular expression patterns in CCR10(EGFP)$^+$ CD3$^-$NK1.1$^+$ immune cells of different tissues and organs. Related to Figures 1 and 2

	Fetal/neonatal thymus[1]	Fetal/neonatal skin[2]	Adult skin[3]	Adult sLN[4]
CCR10	+	+	+	+
CD127	+	+	+	+
CD90	+	+	+	+/-
CD49a	+	+	+/-	+/-
DX5	+	+/-	-	+
NKp46	-	-	+/-	+
CD11b	-	-	-	+/-
IFNγ	+	+	+/-	+
IL-2	+/-	+/-	+	+
TNFα	+/-	+/-	+/-	+/-
Granzyme B	-	-	-	-
B220	+	+	+	+
CD5	-	-	-	-
Gr-1	low/-	-	n.d.	+/-
Eomes	+	+	-	-
PLZF	+	+	-	-

Note: [1]Gated on total thymocytes; [2]Gated on CD45$^+$ lymphocytes; [3]Gated on CD45$^+$ lymphocytes; [4]Gated on total lymphocytes of lymph nodes;
+: >75%, +/-: 75-25%, low/-: 25-10%, -: <10%; n.d.: not determined.

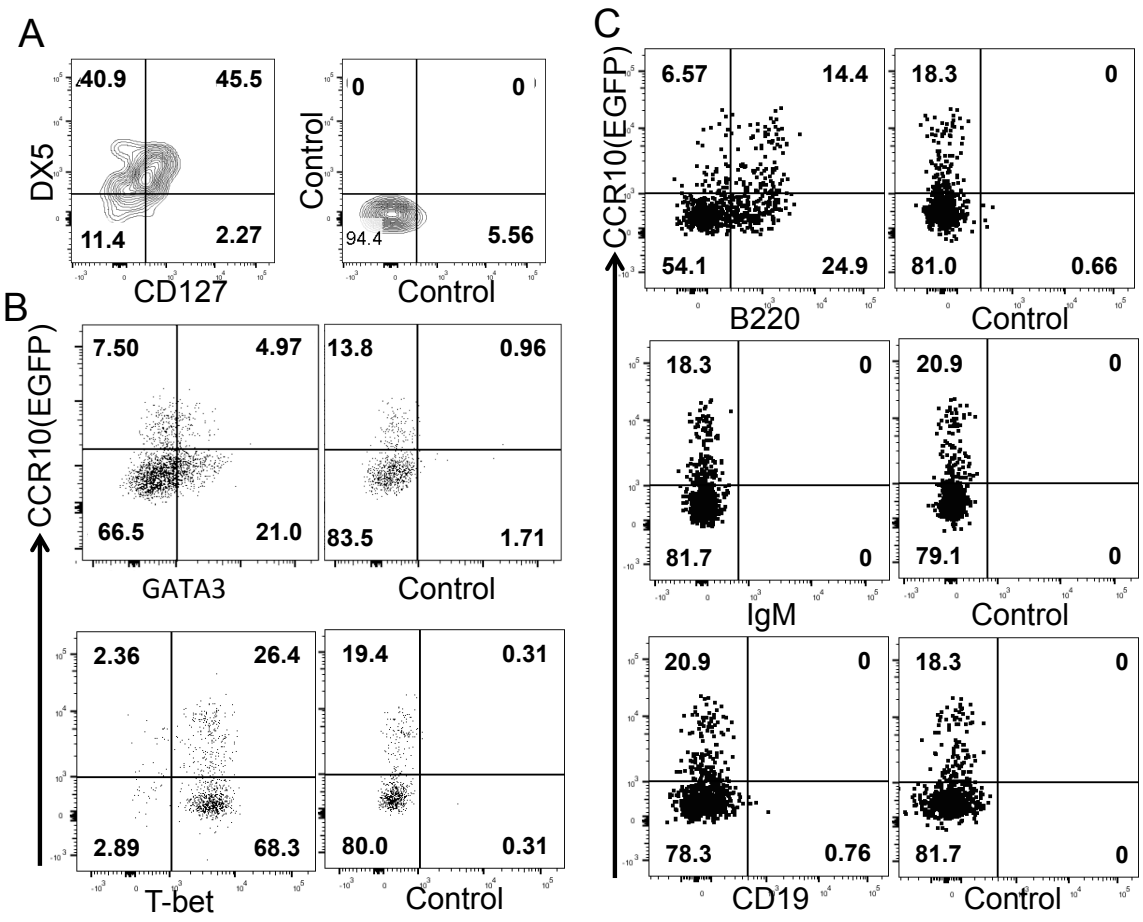

Figure S1. Characterization of CCR10^{+} CD3^{-}NK1.1^{+} thymocytes of neonatal mice. Related to Figure 1. (**A**) Flow cytometric analysis of gated CCR10(EGFP)$^{+}$ CD3^{-} NK1.1^{+} thymocytes of neonatal (1 day-old) CCR10$^{+/EGFP}$ mice for their co-expression of CD127 and DX5 (left). The graph of isotype control antibody staining is shown at the right. (**B**) Flow cytometric analysis of gated CD3^{-}NK1.1^{+} thymocytes of neonatal (1 day-old) CCR10$^{+/EGFP}$ mice for expression of CCR10(EGFP) versus GATA3 or T-bet (left). Graphs of isotype control antibody staining are shown at the right. **(C)** Flow cytometric analysis of gated CD3^{-}NK1.1^{+} thymocytes of neonatal (1 day-old) CCR10$^{+/EGFP}$ mice for their expression of CCR10(EGFP) versus B220, IgM or CD19. Graphs of isotype control antibody staining are shown at the right. B220, IgM and CD19 antibodies are confirmed to be functional based on their positive staining of B cells (not shown).

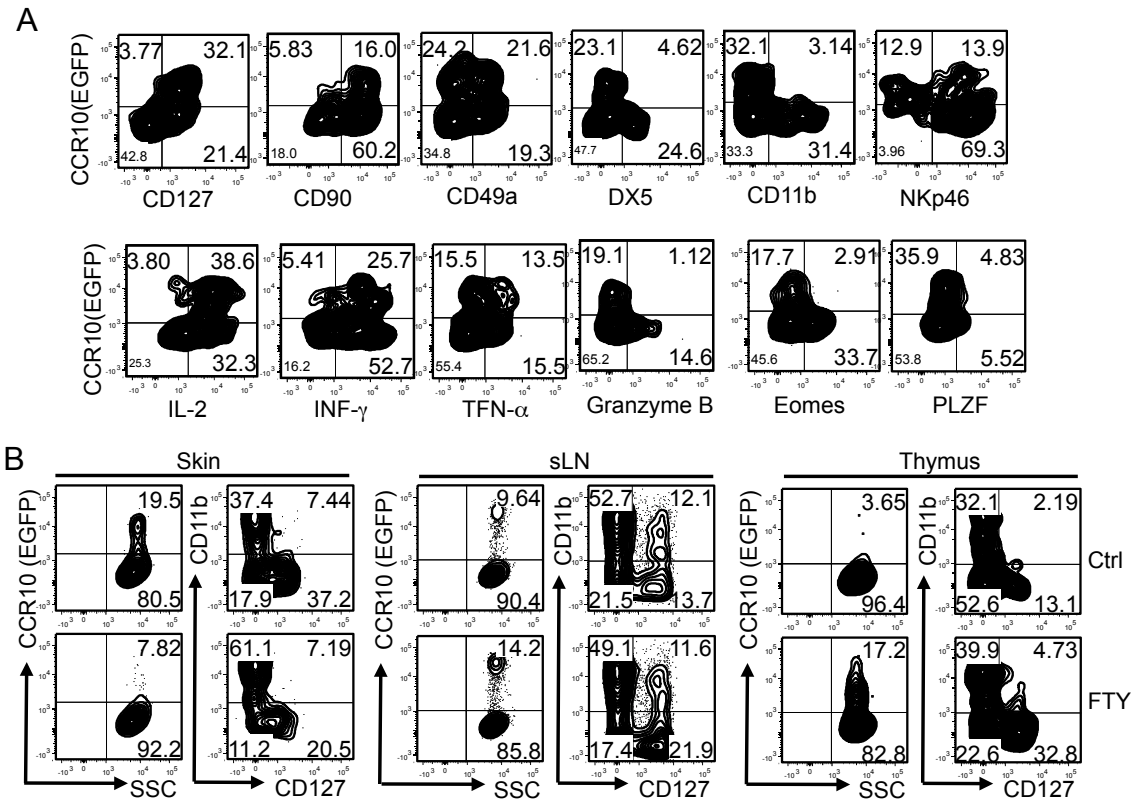

Figure S2. Characterization of CCR10^{+} CD3^{-}NK1.1^{+} lymphocytes of the thymus, sLN and skin of adult mice. Related to Figure 2. (A) Flow cytometric analysis of gated CD3^{-}NK1.1^{+}CD45.2^{+} cells of the skin of adult CCR10$^{+/EGFP}$ mice for their expression of CCR10 (EGFP) and other indicated molecules. Data are representative of at least three experiments. (**B**) Flow cytometric analysis of the expression of CCR10(EGFP), CD127 and CD11b on gated CD3^{-}NK1.1^{+} cells of the skin, sLN and thymus of CCR10$^{+/EGFP}$ mice treated with FTY720 (FTY) or not (Ctrl).

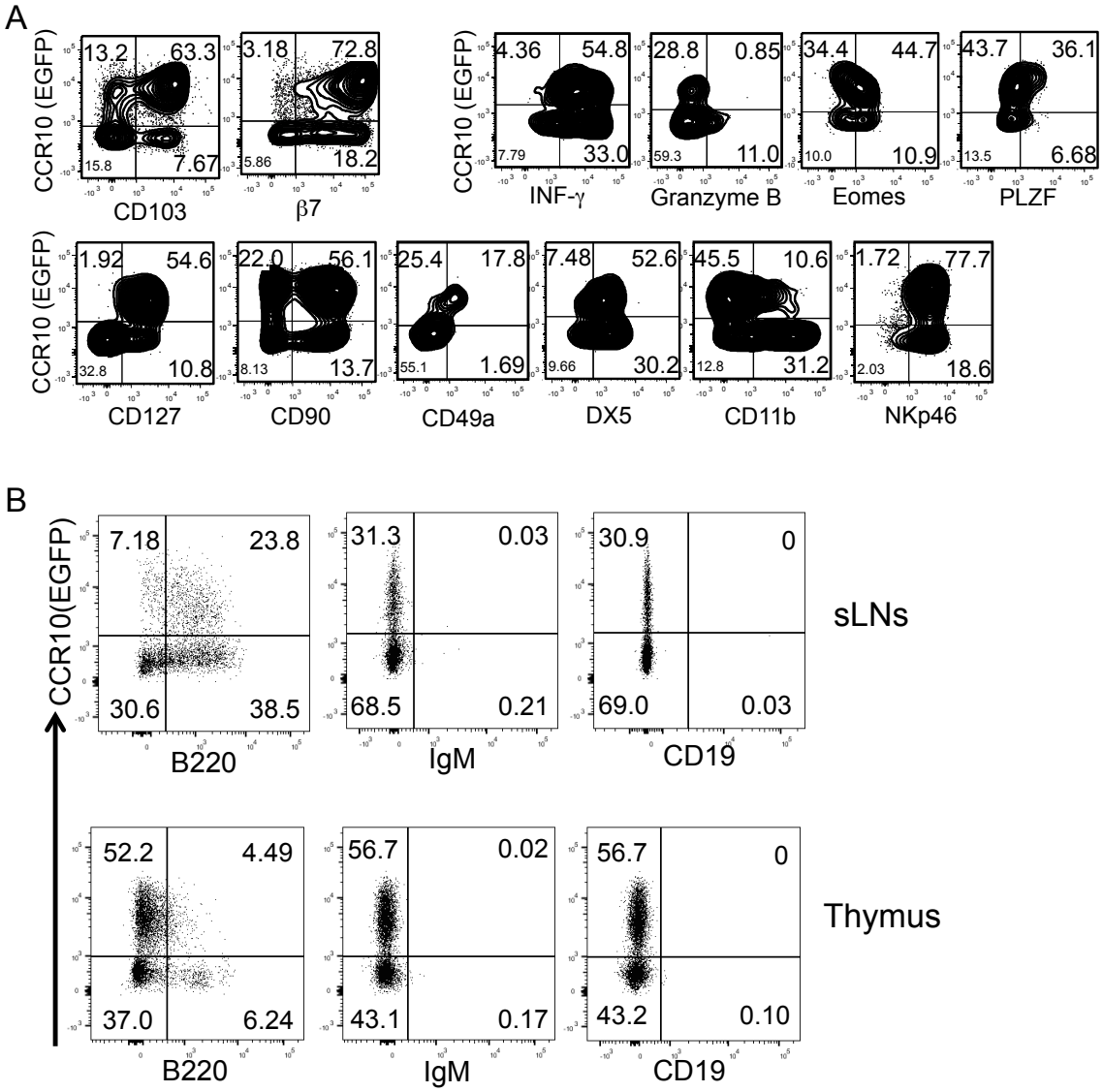

Figure S3. Characterization of CCR10^{+} CD3^{-}NK1.1^{+} lymphocytes of the thymus and sLN of adult Rag1$^{-/-}$CCR10$^{+/EGFP}$ mice. Related to Figure 3. (A) Flow cytometric analysis of gated CD3^{-}NK1.1^{+} thymocytes of adult Rag1$^{-/-}$CCR10$^{+/EGFP}$ mice for their expression of CCR10(EGFP) and other indicated molecules. Data are representative of four experiments. **(B)** Flow cytometric analysis of gated CD45^{+}CD3^{-}NK1.1^{+} cells of skin-draining lymph nodes (sLNs) and thymi of adult Rag1$^{-/-}$CCR10$^{+/EGFP}$ mice for their expression of CCR10(EGFP) versus B220, IgM or CD19.

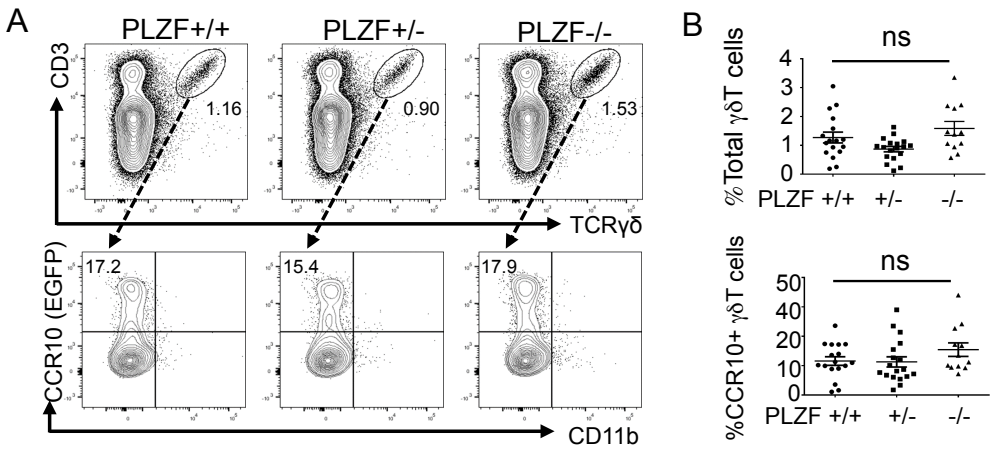

Figure S4. PLZF-knockout does not affect development of total and CCR10^{+} γδT cells in the neonatal thymus. Related to Figure 4. (**A**) Flow cytometric detection of γδT cells (top row) and their expression of CCR10(EGFP) (bottom row) in thymi of neonatal (1-3 day-old) PLZF$^{+/+}$, PLZF$^{+/-}$ and PLZF$^{-/-}$ mice. All mice carry a CCR10-KO/EGFP-KI allele (CCR10$^{+/EGFP}$) for purpose of reporting CCR10 expression with EGFP. (**B**) Comparison of percentages of γδT cells (top) and percentages of them that express CCR10(EGFP) (bottom) in thymi of PLZF$^{+/+}$, PLZF$^{+/-}$ and PLZF$^{-/-}$ neonatal (1-3 day-old) mice. One dot represents one mouse. NS: not significant as determined by two-tailed student's T test.

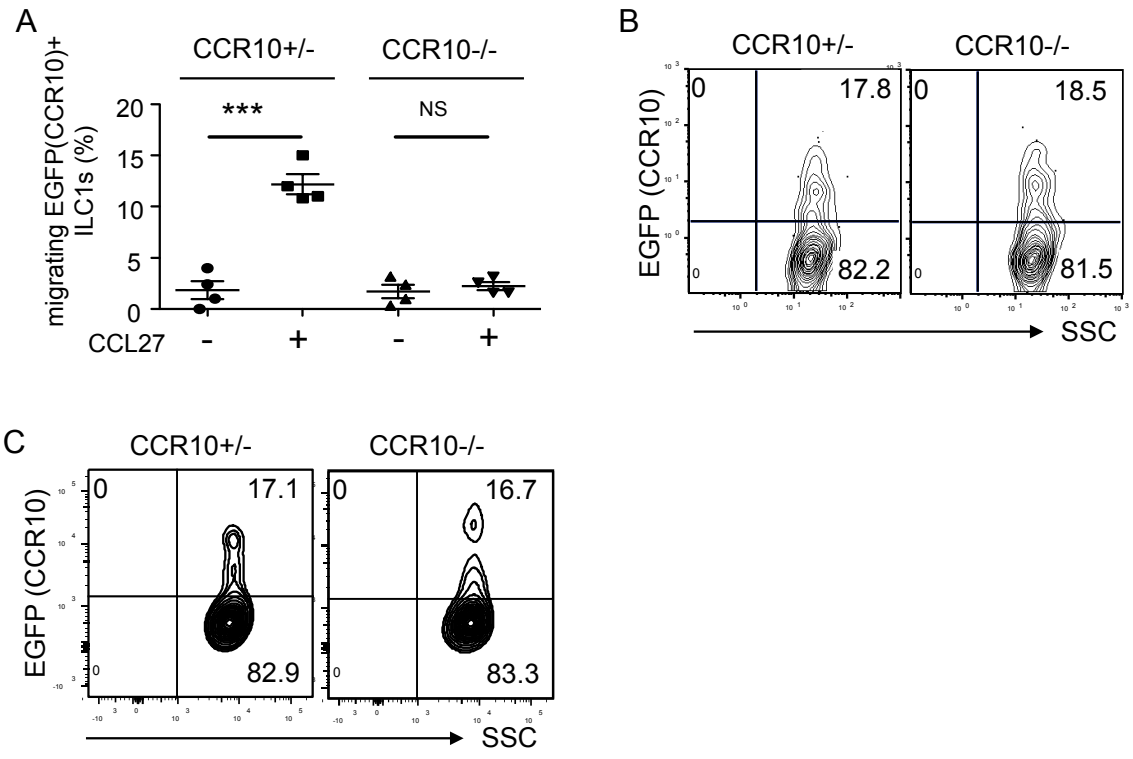

Figure S5. Roles of CCR10 in regulation of migration of CCR10^{+} NK1.1^{+} ILC1s. Related to Figure 4. (**A**) Comparison of the migration efficiency of EGFP(CCR10)$^{+}$ CD3^{-}NK1.1^{+} cells of sLNs of CCR10$^{+/EGFP}$ and CCR10$^{EGFP/EGFP}$ mice towards CCL27 in an *in vitro* transwell migration assay. One dot represents data of one experiment. The percentages are percentages of the EGFP(CCR10)$^{+}$ cells that migrate into bottom wells. ***P<0.001, NS: not significant. (**B, C**) Flow cytometric analysis of EGFP(CCR10)$^{+}$ CD3^{-}NK1.1^{+}CD45^{+} cells in the skin of newborn (B) and adult (C) CCR10$^{+/EGFP}$ and CCR10$^{EGFP/EGFP}$ mice.

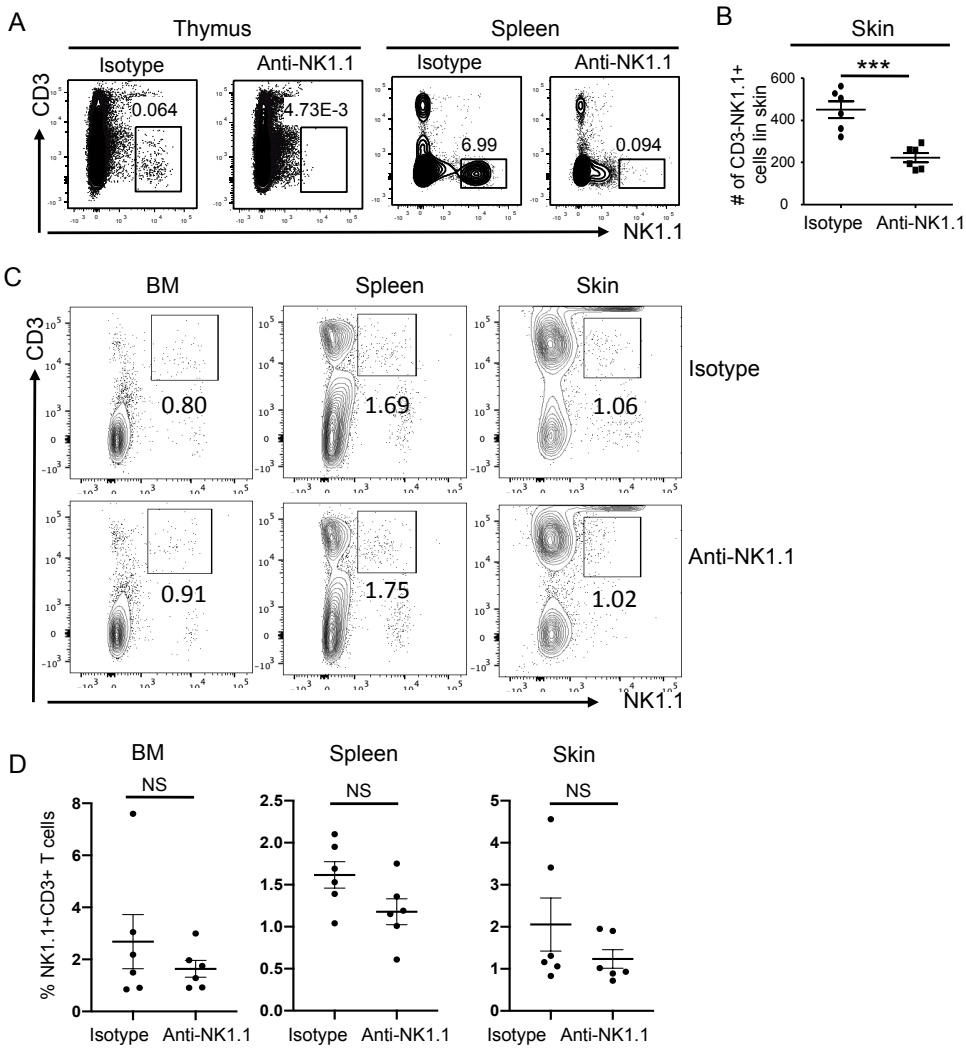

Figure S6. The *in utero* depletion of NK1.1$^+$ ILCs has a lasting effect on establishment of skin NK1.1$^+$ ILCs until young adult ages. Related to Figure 5. (A) Flow cytometric detection of CD3$^-$NK1.1$^+$ cells in thymi and spleens of day 0 newborn mice treated *in utero* at embryonic ages of E13, 15 and 17 with isotype or anti-NK1.1 antibodies injected into pregnant mothers. Data are representative of two independent experiments. (**B**) Comparison of the numbers of CD3$^-$NK1.1$^+$ cells in the skin of 6-week old CCR10$^{+/EGFP}$ mice treated *in utero* with anti-NK1.1 or isotype-matched control antibodies. One dot represents one mouse. (**C**) Flow cytometric detection of NK1.1$^+$CD3$^+$ T cells in gated CD45$^+$ lymphocytes of the BM, spleen and skin of CCR10$^{+/EGFP}$ mice treated *in utero* with anti-NK1.1 or isotype control antibodies. Mice were analyzed 6 weeks after birth. (**D**) Comparison of average percentages of NK1.1$^+$ CD3$^+$ T cells in the BM, spleen and skin of *in utero* anti-NK1.1 and control antibody-treated mice. One dot represents one mouse. ***P<0.001, NS: not significant.

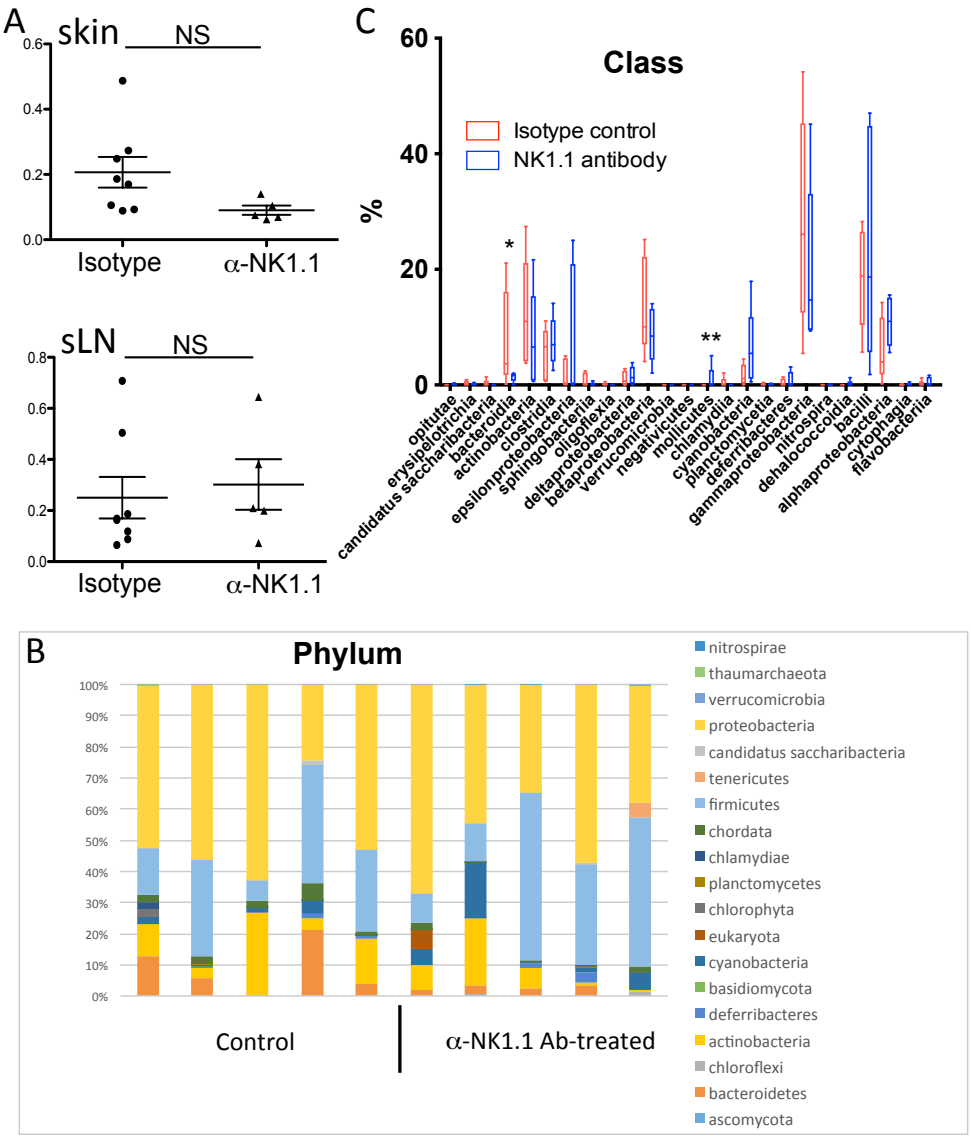

Figure S7. NK1.1^{+} ILC1s play an important role in regulating bacterial colonization in the skin at early postnatal stages. Related to Figure 7. (A) Comparison of relative levels of bacteria in the skin and sLNs of *in utero* anti-NK1.1 and isotype control antibody-treated 9-day-old mice. The levels of bacteria were determined by quantitative PCR analysis of bacterial 16S rRNA genes in genomic DNA isolated from the skin and sLNs. Normalized on GAPDH. One dot represents one mouse. **(B)** Comparison of bacterial phylum compositions in the skin of *in utero* anti-NK1.1 antibody versus control antibody-treated 10-day-old neonatal mice. One bar represents data of one individual mouse. **(C)** Comparison of selective bacterial class compositions in the skin of the *in utero* anti-NK1.1 antibody versus control antibody-treated 10-day-old mice. N=5 skin samples each of anti-NK1.1 antibody and control antibody treated mice. *P<0.05, **P<0.01 based on the Kruskal–Wallis test (Zanvit P, et al. Antibiotics in neonatal life increase murine susceptibility to experimental psoriasis. Nature Communications 6:8424. 2015).

TRANSPARENT METHODS

Mice

CCR10-knockout/EGFP-knockin mice and Vγ43$^{-/-}$ mice were previously described (Jin et al., 2010; Xiong et al., 2008). Rag1$^{-/-}$ and CD45.1^{+} C57BL6 mice were purchased from Jackson Lab (Bar Harbor, ME). PLZF-knockout mice were kindly provided by Drs. Pier Paolo Pandolfi (Beth Israel Deaconess Medical Center) and Derek Sant'Angelo (Rutgers University) (Barna et al., 2000). Rag1$^{-/-}$ and PLZF-knockout mice were crossed with CCR10-knockout/EGFP-knockin mice to introduce one CCR10-knockout/EGFP-knockin allele (CCR10$^{+/EGFP}$) for purpose of reporting CCR10 expression with EGFP. All mice are on the C57BL6 (CD45.2) background and were raised in the SPF conditions unless indicated otherwise. Germ-free C57BL6 mice were obtained from The Pennsylvania State University gnobiotic mouse facility. Both male and female mice were used in the experiments. Sexes of fetal and newborn mice were not determined. All animal experiments were approved by the Institutional Animal Care and Use Committees of the Pennsylvania State University and the University of Texas Health Science Center at San Antonio.

P. aeruginosa skin inoculation

P. aeruginosa (Schroeter) Migula (ATCC# 19660) was grown in Difco nutrient broth (BD) and master stocks were plated overnight on Difco nutrient agar (BD). The following morning, a single colony was grown by shaking in broth at 37°C for 3-4 hours to mid-logarithmic phase as determined by a spectrophotometer. Bacteria were centrifuged at

1500 × *g*, washed in PBS and resuspended in 1-2 mL PBS. Newborn (2-day-old) CCR10$^{+/EGFP}$ littermates were anesthetized with isoflurane and the skin was cleared by tape stripping once prior to topical application of *P. aeruginosa* (5×10^8 CFU in 200 μL PBS) or PBS on the skin of the back and abdomen once a day for two consecutive days. Five days after inoculation, pups were euthanized and the skin and sLNs were harvested for flow cytometric analysis.

Reagents

Anti-mouse CD122 (Clone# TM-b1), anti-mouse NKp46 (29A1.4), anti-mouse CD90.2 (53-2.1), anti-mouse granzyme B (Clone# NGZB) anti-mouse Eomes (Dan11mag) and anti-mouse Sca-1 (D7) antibodies were purchased from eBioscience (San Diego, CA). Anti-mouse IL-17A (TC11-18H10.1), anti-mouse CD45.1 (A20), anti-mouse CD45.2 (104), anti-mouse CD3ε (145-2C11 or 17A2), anti-mouse CD103 (2E7), anti-mouse CD127 (A7R34), anti-mouse β7 (FIB504), anti-mouse CD49b (DX5), anti-mouse CD11b (M1/70), anti-mouse c-kit (2B8), anti-mouse CD49a (HMa1), anti-mouse TNF-α (MP6-XT22), anti-mouse B220 (RA-3-6B2), anti-mouse Gr-1 (RB6.8C5), anti-mouse CD5 (53-7.3), anti-mouse PLZF (9E12) and anti-mouse granzyme C (SFC1D8) were purchased from Biolegend (San Diego, CA). Anti-mouse IFNγ (XMG1.2), anti-mouse NK1.1 (PK136), anti-mouse α4β7 (DATK32) and PE-CF594-Streptavidin were purchased from BD Biosciences (San Jose, CA). A cocktail of antibodies against the lineage (Lin) markers [CD5, CD45R (B220), CD11b, Gr-1 (Ly-6G/C), 7-4, and Ter-119 antibodies] and anti-biotin microbeads were purchased from Miltenyi Biotec (San Diego, CA). FTY720 was purchased from Cayman chemical (Ann Arbor, Michigan). Anti-NK1.1

antibody for depletion (PK136) and mouse IgG2a isotype control (BE0085) were purchased from Bio X Cell (West Lebanon, NH).

Cell isolation

Isolation of lymphocytes from the skin and lamina propria of intestines was performed as previously described (Hu et al., 2011; Xia et al., 2014). BM cells were collected from tibias and femurs. Thymic, liver, splenic and lymph node cells were prepared by pressing the tissues through cell strainers using the end of a sterile plunger of a 10-ml syringe. For isolation of lymphocytes from livers, dissociated liver cells were resuspended in 3 mL of 80% Percoll (GE Healthcare), underlaid with 4 mL of 40% Percoll, and centrifuged for 20 min at 850 × *g* at room temperature. Lymphocytes were recovered from the interphase of the Percoll gradient after the centrifugation, washed and resuspended in a staining buffer (PBS containing 3% FBS) for further analysis.

Cell staining, flow cytometric analysis and cell sorting

For surface molecule staining, cells were incubated with primary antibodies in staining buffer for 25 min at 4°C, and if necessary, with secondary antibodies for 15 min at 4°C. For intracellular molecular staining, cells were fixed with 4% paraformaldehyde and permeabilized with permeabilization buffer from eBioscience, and then resuspended in permeabilization buffer with antibodies. To detect cytokines and granzyme B, cells were first stimulated with PMA (1 μg/mL) and inomycin (2 μg/ mL) (both from Millipore Sigma) for 3 hours in presence of brefeldin A (1 μg/mL) and then were stained for extracellular and intracellular proteins. To detect intrinsic granzyme C expression, cells

were cultured for 3 hours in presence of brefeldin A (1 μg/mL) without PMA/ionomycin stimulation and then were stained for extracellular and intracellular proteins. Flow cytometric analyses were performed on FC500 (Beckman Coulter) or BD Fortessa LSRII (BD Biosciences). Data were analyzed with FlowJo software (FlowJo LLC., Ashland, OR). Cell sorting was performed using BD Cytopeia's Influx (BD Biosciences) or MoFlo Astrios (Beckman Coulter).

Adult bone marrow and fetal liver reconstitution

$CD45.1^+$ adult BM cells and $CD45.2^+$ E16 fetal liver cells were co-injected intravenously into lethally irradiated (950 rad) $CD45.1^+CD45.2^+$ WT C57BL/6 mice. Recipients were analyzed 8 weeks after injection of the cells.

***In utero* antibody depletion of $NK1.1^+$ cells**

Pregnant mice were injected intravenously at E13, E15 and E17 with anti-NK1.1 or isotype control antibodies (500 μg/injection). The efficiency of depletion was assessed on cells of the thymus and spleen of newborn pups of antibody-treated mothers.

FTY720 treatment

Mice were treated with 10 μg/mL FTY720 in drinking water for 2 weeks.

***In vitro* migration assay of $CCR10^+$ cells to CCL27**

The experiment was performed similarly as previously described (Xiong et al., 2004). Briefly, $CCR10^{+/EGFP}$ and $CCR10^{EGFP/EGFP}$ skin-draining lymph node cells were placed

into the upper chamber of a Transwell plate containing a 5-μm pore filter and incubated with medium only or medium containing CCL27 in the bottom chamber for four hours. Cells in the top chamber and migrating into the bottom chamber were then collected and analyzed by flow cytometry, based on which percentages of EGFP(CCR10)$^{+}$ CD3^{-} NK1.1^{+} cells that migrated into bottom chambers were calculated.

Statistical analyses

Paired or unpaired two-tailed student T tests were used for statistical analysis in most experiments. The Kruskal–Wallis test was used for comparison analysis of bacterial composition differences in the skin of *in utero* anti-NK1.1 versus isotype control antibody-treated mice (Zanvit et al., 2015). $P < 0.05$ was considered significant.

Reference

Barna, M., Hawe, N., Niswander, L., and Pandolfi, P.P. (2000). Plzf regulates limb and axial skeletal patterning. Nat Genet *25*, 166-172.

Hu, S., Yang, K., Yang, J., Li, M., and Xiong, N. (2011). Critical roles of chemokine receptor CCR10 in regulating memory IgA responses in intestines. Proc Natl Acad Sci U S A *108*, E1035-1044.

Jin, Y., Xia, M., Sun, A., Saylor, C.M., and Xiong, N. (2010). CCR10 is important for the development of skin-specific gammadeltaT cells by regulating their migration and location. J Immunol *185*, 5723-5731.

Xia, M., Hu, S., Fu, Y., Jin, W., Yi, Q., Matsui, Y., Yang, J., McDowell, M.A., Sarkar, S., Kalia, V., *et al*. (2014). CCR10 regulates balanced maintenance and function of resident regulatory and effector T cells to promote immune homeostasis in the skin. J Allergy Clin Immunol *134*, 634-644 e610.

Xiong, N., Kang, C., and Raulet, D.H. (2004). Positive selection of dendritic epidermal gammadelta T cell precursors in the fetal thymus determines expression of skin-homing receptors. Immunity *21*, 121-131.

Xiong, N., Zhang, L., Kang, C., and Raulet, D.H. (2008). Gene placement and competition control T cell receptor gamma variable region gene rearrangement. J Exp Med *205*, 929-938.

Zanvit, P., Konkel, J.E., Jiao, X., Kasagi, S., Zhang, D., Wu, R., Chia, C., Ajami, N.J., Smith, D.P., Petrosino, J.F., *et al*. (2015). Antibiotics in neonatal life increase murine susceptibility to experimental psoriasis. Nat Commun *6*, 8424.